Phase separation, ferromagnetism and magnetic irreversibility in La$_{1-x}$Sr$_x$Mn$_{1-y}$Fe$_y$O$_3$

V.S. Zakhvalinskii [a,b], R. Laiho [c], A.V. Lashkul [a], K.G. Lisunov [a,d], E. Lähderanta [a,*],
Yu.S. Nekrasova [b], P.A. Petrenko [d]

[a] Department of Mathematics and Physics, Lappeenranta University of Technology, PO Box 20, FIN-53851 Lappeenranta, Finland
[b] Department of Physics, Belgorod State University, RUS-308015 Belgorod, Russia
[c] Wihuri Physical Laboratory, University of Turku, FIN-20014 Turku, Finland
[d] Institute of Applied Physics ASM, Academiei Str. 5, MD-2028 Kishinev, Moldova

ARTICLE INFO

ABSTRACT

Magnetic susceptibility, $\chi(T)$, is investigated in ceramic La$_{1-x}$Sr$_x$Mn$_{1-y}$Fe$_y$O$_3$ (LSMFO) samples with $x=0.3$ and $y=0.15-0.25$. A ferromagnetic (FM) transition observed in LSMFO is accompanied with an appreciable decrease of the transition temperature with increasing y, which is connected to breaking of the FM double-exchange interaction by doping with Fe. Strong magnetic irreversibility, observed in low ($B=10$ G) field, gives evidence for frustration of the magnetic state of LSMFO. The FM transition, which is expanded with increasing B, is more pronounced in the samples with $y=0.15-0.20$ and broadens considerably at $y=0.25$, where the irreversibility is increased. Well above the transition, $\chi(T)$ exhibits a Curie–Weiss asymptotic behavior, yielding very large values of the effective Bohr magneton number per magnetic ion, incompatible with those of Mn or Fe single ions. At $y=0.15$ and 0.20 a critical behavior of $\chi^{-1}(T)\sim(T/T_C-1)^\gamma$ in the region of the FM transition is characterized by influence of two different magnetic systems, a 3D percolative one with $\gamma=\gamma_p \approx 1.8$ and $T_C=T_C^{(p)}$, and a non-percolative 3D Heisenberg spin system, with $\gamma=\gamma_H \approx 1.4$ and $T_C=T_C^{(H)}$, where $T_C^{(p)} < T_C^{(H)}$. At $y=0.25$ the percolative contribution to the critical behavior of $\chi(T)$ is not observed. The dependence of χ on T and y gives evidence for phase separation, with onset already near the room temperature, leading to generation of nanosize FM particles in the paramagnetic host matrix of LSMFO. The ferromagnetism of LSMFO is attributable to percolation over the system of such particles and generation of large FM clusters, whereas the frustration is governed presumably by a system of smaller weakly-correlated magnetic units, which do not enter the percolative FM clusters.

© 2011 Elsevier B.V. All rights reserved.

1. Introduction

La$_{1-x}$Sr$_x$Mn$_{1-y}$Fe$_y$O$_3$, briefly LSMFO, belongs to a family of hole-doped mixed-valence manganite perovskites, exhibiting a colossal magnetoresistive effect (CMR) [1]. The compound is obtained by substitution of Fe for Mn in La$_{1-x}$Sr$_x$MnO$_3$ (LSMO) [2]. The hole doping of manganite perovskites, realized by substitution of a divalent element for La^{3+} or by formation of cation vacancies, introduces, besides Mn^{3+}, a fraction of Mn^{4+} ions [3]. The Mn$^{3+,4+}$ mixed valence leads to ferromagnetic (FM) Mn$^{3+}-$Mn^{4+} double-exchange (DE) interactions, competing with antiferromagnetic (AF) Mn$^{3+}-$Mn^{3+} superexchange (SE) interactions [3]. However, the SE$-$DE competition, proposed for interpretation of the magnetic phases of manganite perovskites [4], cannot explain the whole variety of the electronic and magnetic properties of these materials. Further investigations have emphasized the importance of the interplay between charge, spin and orbital degrees of freedom [5], as well as the crucial role of phase separation in the physics of manganite perovskites and related CMR compounds [6].

Experimental evidence for different phases, metallic and insulating, as well as FM and paramagnetic (PM) or AFM, coexisting in one and the same compound, has been obtained in a broad variety of the manganite perovskites (see e. g. [7–12]). Theoretical investigations, using various approximations of the model Hamiltonian, have yielded diagrams of coexisting phases, demonstrating the instability of a homogeneous electronic phase and breaking of macroscopic fractions of different phases into mixtures of nanosize regions (see [5,6] and references therein). These investigations prove that phase separation is an intrinsic property of manganites, irrespective of chemical or compositional inhomogeneity of the material. Another important feature is the percolative character of the coexisting phases [7,10,11,13], which is quite sensitive to external influence [6]. A high sensitivity of the phase ratio to the temperature, T, and the applied magnetic field, B, has been established as well, including increase of the fraction of the FM (metallic) phase with increasing B or decreasing T [6,14,15]. At this point, a special temperature scale,

T^*, has been proposed to characterize the onset of the phase separation in manganites [6].

Investigations of LSMFO have revealed a high sensitivity of magnetic and transport properties to Fe doping [16–20]. In particular, it has been established a strong decrease of the FM Curie temperature, T_C, with y, attributable to two different reasons [20]. The first one is connected to a direct replacement of Mn^{3+} by Fe^{3+} ions [21], which do not support the DE interactions in the $Fe^{3+}-Mn^{4+}$ pairs [16,22]. The second reason is increasing microscopic disorder due to Fe doping [20]. Although both effects are possible (as found e. g. in $La_{1-x}Ca_xMn_{1-y}Fe_yO_3$ [23]), their influence on the dependence of T_C on y in LSMFO remains unclear. Another interesting feature of LSMFO is the magnetic irreversibility, pertinent to frustrated systems such as spin-glasses or cluster-glasses [24], and observed together with the FM transition [20]. Coexistence of the FM and glassy properties has been found in many other manganite perovskites like $La_{1-x}Ca_xMnO_3$ [25], $La_{1-x}Ca_xMn_{1-y}Fe_yO_3$ [23], $La_{1-x}Ba_xMnO_3$ [26], $Nd_{0.7}Sr_{0.3}MnO_3$ [27] and $Y_{0.7}Ca_{0.3}MnO_3$ [28], although its connection to the phase separation is not understood well enough.

Simultaneous investigations of the FM transition and the magnetic irreversibility should be made in low magnetic fields, when the perturbation of the spin system is minimal. In this paper are presented and discussed measurements of the magnetization in LSMFO in fields between 10 G–1 kG, to obtain information on the role of the phase separation in formation of a microscopic magnetic state at different levels of Fe doping.

2. Results and discussion

2.1. Experimental details

LSMFO samples with $x=0.3$ and $y=0.15$ (#15), 0.20 (#20) and 0.25 (#25) were synthesized with the conventional solid-state reaction method, similar to preparation of $La_{1-x}Ca_xMnO_3$ [25], from La_2O_3, MnO_2, Fe_2O_3 and $SrCO_3$. The starting materials were pre-calcined to remove possible adsorbates, weighted in stoichiometric proportions and mixed with subsequent heating in air at 1360 °C for 40 h and intermediate grindings. The mixtures were pressed into pellets and fired in air at 1500 °C for 22 h. According to x-ray diffraction data all samples had the rhombohedrally distorted structure (space group R-3c) with lattice parameters $a=5.508(4)$, 5.513(2) and 5.513(4) Å and $c=13.365(6)$, 13.360(4) and 13.376(7) Å for $y=0.15$, 0.20 and 0.25, respectively.

Composition and distribution of the elements in the samples were investigated by the microprobe and the scanning–tunneling microscopy methods. The grains size of the LSMFO samples was a few micrometers and the distribution of the elements over the volume of the samples and separate grains was homogeneous and stoichiometric.

Magnetization, $M(T)$, was measured with an RF-SQUID mag-netometer after cooling the sample from the room temperature down to 3 K in zero magnetic field (M_{ZFC}) or in fields of 10 G, 0.5 kG and 1 kG (M_{FC}). Temperature dependence of the thermo-remanent magnetization (TRM) was measured after cooling the sample from the room temperature down to 3 K in the field of 10 G and then reducing the field to zero.

2.2. Ferromagnetic transition in LSMFO

As evident in Fig. 1, both $\chi_{ZFC}(T)$ and $\chi_{FC}(T)$ (where $\chi=M/B$) exhibit at $B=10$ G a steep increase with lowering of T, typical of a FM transition. The transition temperature, T_C, can be defined primarily by the inflection point of the $\chi(T)$ curves, denoted below as $T_C^{(inf)}$. The transition width can be characterized by the width of the plots of $d\chi_{ZFC}(T)/dT$ and $d\chi_{FC}(T)/dT$ vs. T as shown in Fig. 2. The
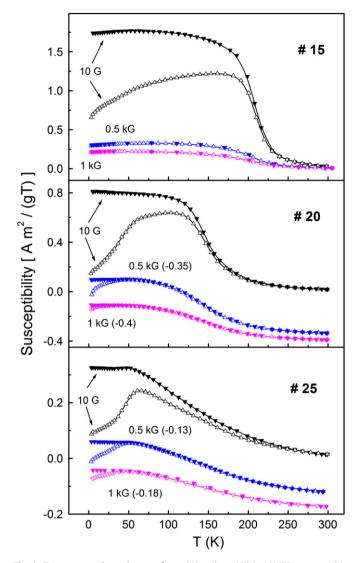

Fig. 1. Temperature dependences of χ_{ZFC} (Δ) and χ_{FC} ($\blacktriangledown$) in LSMFO, measured in various magnetic fields. Some of the plots are shifted along the vertical axis by the values given in parenthesis.

values of $T_C^{(inf)}$ are obtained from the minimum of these curves and the dependence of $T_C^{(inf)}$ on y is presented in the inset of Fig. 2. The transition is well-determined for #15 and #20, but is broaden considerably in #25, suggesting ferromagnetism of LSMFO below $T_C^{(inf)}$ in the interval of $y=0.15$–0.20, and a border of the FM part of the (T, y) magnetic phase diagram of LSMFO near $y \approx 0.25$. A noticeable feature of the plots in Fig. 1 is the increase in the width of the FM transition with increasing B. This behavior is attributable to phase separation and increase of the hole-rich FM phase, embedded in the PM host matrix, which is sensitive to the applied magnetic field (Section 1).

The dependence of T_C on y can be analyzed with the Varma model [29], which treats the PM−FM transition of the manganites by considering the magnetic disorder and the localization of the elec-trons inside a band of width W. This model is applied to interpret T_C e.g. in LSMO [29], $La_{1-x}Ca_xMnO_3$ [25], $LaMnO_{3+\delta}$ [30], $La_{1-x}Ba_xMnO_3$ [26] and $LaMn_{1-x}Ni_xO_3$ [31]. In low fields minimizing the effect of the phase separation, T_C is given by the expression

$$kT_C \approx 0.05\,Wc(1-c) \qquad (1)$$

where c is the concentration of the holes or Mn^{4+} [29]. Taking into account that Fe^{3+} ions do not support the FM DE interactions [16,22] and substitute directly Mn^{3+} in the lattice of manganites [21], as well
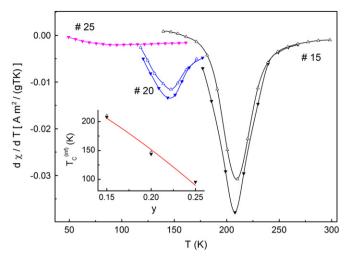
Fig. 2. Temperature dependences of dχ_{ZFC}/dT ($\triangle$) and dχ_{FC}/dT ($\blacktriangledown$) in the LSMFO samples at $B = 10$ G. The lines are to guide the eye. Inset: the dependence of $T_C^{(inf)}$ on y, obtained in the ZFC ($\triangle$) and FC ($\blacktriangledown$) regimes of cooling.

as that doping with Fe causes minor lattice distortions due to similar ionic radii of Fe^{3+} and Mn^{3+} [22], we can use Eq. (1) for quantitative interpretation of $T_C(y)$ by putting $c \approx c_0 - y$ [23]. Here c_0 is the value of c at $y = 0$, expected to be close to x. More strictly, $c_0 - x$ is determined by the hole doping, connected only to the cation vacancies (Section 1). The fit of $T_C^{(inf)}(y)$, given by the solid line in the inset to Fig. 2, yields the values of $W = 2.6 \pm 0.1$ eV and $c_0 = 0.31 \pm 0.01$, showing that c_0 can differ from $x = 0.30$ only by $\sim 3 - 6\%$, which are typical values of the relative hole concentration due to the cation vacancies in manganites [30]. On the other hand, W, obtained above, coincides within the error with the value of $W \approx 2.5$ eV given for LSMO [29]. Hence, the decay of T_C in LSMFO between $y = 0.15 - 0.25$ is determined mainly by breaking of the DE interactions by Fe^{3+}, whereas the disorder caused by the Fe doping plays a negligible role. Instead, in $La_{1-x}Ca_xMn_{1-y}Fe_yO_3$ $T_C(y)$ is influenced strongly by the disorder [23] and the Fe doping induces an additional fluctuating short-range potential, contributing to the microscopic disorder at $y \geq 0.03$ [32].

2.3. Magnetic irreversibility phenomena in LSMFO

An important feature of the magnetic behavior of LSMFO, following from the plots in Fig. 1 for #15 and #20, is the irreversibility or the deviation of $\chi_{ZFC}(T)$ from $\chi_{FC}(T)$ with the onset near the FM transition. On the other hand, in #25 one can see a substantial shift of the onset of the irreversibility from T_C towards higher temperatures. Other noticeable features are the relatively weak temperature dependence of $\chi_{ZFC}(T)$ within a broad interval below T_C in #15. Similar behavior of $\chi_{ZFC}(T)$ is observed in #20, but persisting only down to ~ 60 K, with subsequent rapid decrease when T is decreased, and a rounded peak of $\chi_{ZFC}(T)$, observed in #25 below T_C instead of the plateau. The magnetic irreversibility is most pronounced in the field of 10 G, disappears in #15 at $B = 0.5$ kG and is almost suppressed in #20 at $B = 1$ kG, whereas in #25 a clear difference between $\chi_{ZFC}(T)$ and $\chi_{FC}(T)$ is observed below 50 K even in the field of 1 kG (Fig. 1). As can be seen in the top panel of Fig. 3, the temperature dependence of TRM/B follows reasonably the difference of $\chi_{FC}(T) - \chi_{ZFC}(T)$ in #25, but deviates systematically from this difference in #15 and #20 within the intervals, corresponding approximately to those of the weak temperature dependence of $\chi_{ZFC}(T)$ in Fig. 1.

The irreversible magnetic behavior in Figs. 1 and 3 indicates a frustrated magnetic state in LSMFO. Such behavior is pertinent to spin-glass (SG) or cluster-glass (CG) phases below the onset of
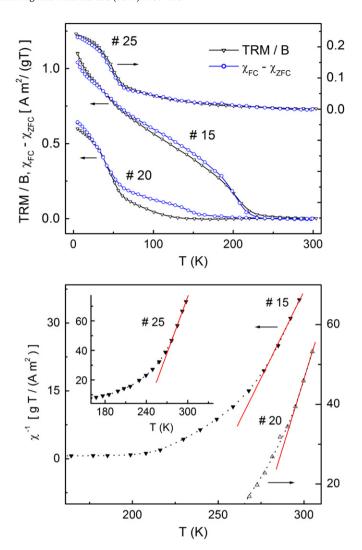

Fig. 3. Plots of TRM/B vs. T ($\triangledown$) and $\chi_{FC} - \chi_{ZFC}$ vs. T ($\circ$) (top panel) and temperature dependences of χ^{-1} in the ZFC ($\triangle$) and FC ($\blacktriangledown$) regimes of cooling (bottom panel) for the LSMFO samples at $B = 10$ G. The solid lines are linear fits and the dotted lines are to guide the eye.

freezing-in of the magnetic moments, where the frustration is connected to competing interactions between the moments [24]. In the SG phase, the expression

$$\text{TRM}(T) = M_{FC}(T) - M_{ZFC}(T) \qquad (2)$$

is expected, reflecting a symmetry of the energy distribution of potential barriers in the presence or absence of the external magnetic field [25,33,34]. In the CG phase this symmetry may be broken due to the anisotropy, associated with the shape and orientation of the clusters [33,34], leading to violation of Eq. (2).

Hence, a good coincidence of the left- and right-hand parts of Eq. (2) for #25 (top panel of Fig. 3), accompanied by the rounded maximum of $\chi_{ZFC}(T)$ in the bottom panel of Fig. 1 and a poor FM behavior (very broad minimum of dχ/dT in Fig. 2), suggests that the magnetic state of #25 is governed presumably by a system of weakly-correlated independent carriers of the magnetic moment, such as single magnetic ions and/or relatively small FM clusters. On the other hand, violation of Eq. (2) for #15 and #20 (Fig. 3) within the intervals, which are close to those of the weak temperature dependence of $\chi_{ZFC}(T)$ in Fig. 1, is more typical of the frustrated FM phase. Accompanied with the well-determined FM transition in Fig. 2, such behavior implies an important role of large and strongly-correlated

FM clusters, attributable to percolation over a system of hole-rich FM particles. However, in the top panel of Fig. 3 one can see that the violation of Eq. (2) for #20 and especially for #15 is not strong, without qualitative differences between TRM $(T)/B$ and $\chi_{FC}(T) - \chi_{ZFC}(T)$. This suggests that the system of the relatively small and weakly-correlated magnetic units, like in #25, is responsible for the irreversibility and frustration in #15 and #20 as well, coexisting with the large percolative clusters governing the FM properties. In turn, strong expansion of the FM transition and weakening of the FM properties means that large FM clusters have no influence on magnetic behavior of #25.

2.4. Magnetic properties of LSMFO above T_C

As shown in the bottom panel of Fig. 3 the inverse suscept-ibility tends asymptotically to the Curie–Weiss dependence (solid lines), given by the law $\chi(T) = C/(T - \theta)$, provided that the short-range FM fluctuations can be neglected well above the FM transition. Here $C = p_{eff}^2 \mu_B^2 N/(3k)$ is the Curie constant, p_{eff} is the effective Bohr magneton (μ_B) number per magnetic ion, N is the concentration of the magnetic ions and θ is the Weiss tempera-ture. The linear fit of the plots of χ^{-1} vs. T in the ZFC and FC regimes above $T \approx 277$–278 K yield the values of $p_{eff}^2 \approx 240$–280, 280–300 and 140–180 for #15, #20 and #25, respectively, if N is taken equal to the concentration $N_0 = 1.42 \times 10^{22}$ cm^{-3} of the Mn sites (or, equivalently, to the total concentration of magnetic ions in LSMFO). It can be seen that p_{eff}^2 exceeds considerably the values of $p_{eff}^2 \approx 24$, 15 and 35, for single Mn^{3+}, Mn^{4+} and Fe^{3+} ions, respectively. The large deviation from the single-ion values of p_{eff} implies that the phase separation in LSMFO takes place already well above the FM transition, whereas the scale T^*, introduced in [6] for the onset of the phase separation, exceeds even the room temperature. A similar situation was observed in La$_{1-x}$Ba$_x$MnO$_3$, but with much smaller difference between experimental values of $p_{eff}^2 = 33$–40 and the value of $p_{eff}^2 \approx 22$, expected for a mixture of Mn^{3+} and Mn^{4+} ions in this compound [26].

Eventually, interesting information about the magnetic phases of LSMFO can be obtained from critical behavior of $\chi(T)$ near the FM transition, violating the Curie–Weiss law (bottom panel of Fig. 3) with decreasing the temperature. Such behavior is given by the law $\chi(T) \sim (T/T_C - 1)^{-\gamma}$, where γ is the critical exponent depending on the nature and the dimensionality of the spin system [36]. For the analysis of the experimental data it is convenient to use the following equivalent forms,

$$c^{-1} - \chi c^{-1} \sim \tau^\gamma \quad \text{and} \quad d\chi^{-1}/dT \sim \tau^{\gamma-1} \tag{3}$$

where $\tau = T/T_C - 1$. The term $\chi_C^{-1} = \chi^{-1}(T_C)$ is introduced in the first of Eq. (3) to account for a (non-magnetic) inhomogeneity of the material, leading to a finite non-zero value of the inverse susceptibility at T_C. The second of Eq. (3) has some advantage for applications, because it does not contain the additional terms like the first one, making the analysis more straightforward. However, differentiation may be a source of an additional error, connected to an increased scattering of the experimental points.

The dependences of $\ln(\chi^{-1} - \chi_C^{-1})$ on $\ln \tau$ were determined by interpolation of $\chi(T)$ and variation of T_C with a step of 0.5–1 K, to achieve the minimum standard deviation (SD) of the linear fits to the plots, evaluated at different T_C. The SD minimum as the criterion of the best fit was used for the plots of $\ln(d\chi^{-1}/dT)$ vs. $\ln \tau$, as well, varying T_C with the same step. The procedure above yielded the pairs of T_C and γ or T_C and $\gamma - 1$, applying the first or the second of Eq. (3), respectively, and the optimum temperature interval, corresponding to the minimum of SD vs. T_C plots.

The formal dependences of SD and γ on T_C, as well as those of SD and $\gamma - 1$ on T_C are shown, for some selected cases, in Figs. 4 and 5, respectively. In the insets are displayed the plots

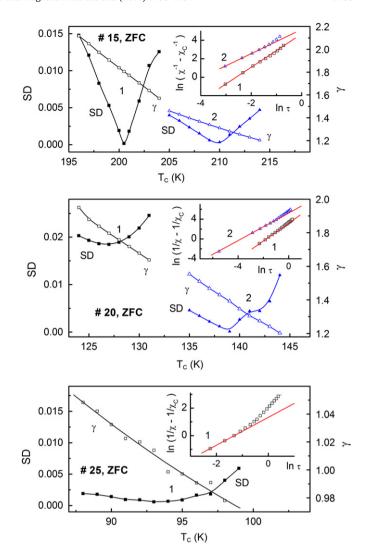Fig. 4. Dependences of SD and γ on T_C, obtained within the temperature intervals ΔT_1 (1) and ΔT_2 (2), with the first of Eq. (3). The lines are to guide the eye. Insets: plots of $\ln(\chi^{-1} - \chi_C^{-1})$ (in arbitrary units) vs. $\ln \tau$ in the intervals ΔT_1 (1) and ΔT_2 (2) for the LSMFO samples at $B = 10$ G. The lines are linear fits.

of $\ln(\chi^{-1} - \chi_C^{-1})$ vs. $\ln \tau$ and $\ln(d\chi^{-1}/dT)$ vs. $\ln \tau$, evaluated with the pairs of T_C and γ at the SD minimum. The analysis has been extended to all the data in Fig. 1 at $B = 10$ G. The values of T_C and γ, found within the optimum temperature intervals, ΔT, in both conditions of cooling and applying the first (f) and the second (s) of Eq. (3), are collected in Table 1.

The analysis of the critical behavior of the susceptibility in #15 and #20 with the first of Eq. (3) yields two minima of SD (T_C) (Fig. 4), corresponding to two different values of T_C and γ, marked in Table 1 as $T_C^{(1)}$, γ_1, $T_C^{(2)}$ and γ_2, respectively. Some ambiguity of the results, connected to the overlap of the optimum intervals ΔT_1 and ΔT_2 in Table 1, does not look significant, because the SD vs. T_C plots are well-separated. In addition, the values of $T_C^{(j)}$ and γ_j ($j = 1$ and 2) are reproduced with good accuracy with the analysis, based on the second of Eq. (3) and shown in Fig. 5 (cf. the lines f and s in Table 1). It can be seen that $T_C^{(1)} < T_C^{(2)}$, whereas the values of γ_1 and γ_2 lie close to $\gamma_P = 1.70$–1.80 [36,37] and to $\gamma_H = 1.39$ [35,38], respectively, as predicted for a 3D percolation system and for a 3D Heisenberg spin system, respectively.

In #25 a single SD minimum (see bottom panel of Fig. 4), found with the first of Eq. (3), is accompanied with a large difference between the values of γ found in the ZFC and FC regimes (Table 1, lines f), which in turn are close neither to γ_P nor

to γ_H. The more definite results are obtained by analyzing the derivative with the second of Eq. (3), yielding γ_2 around γ_H and γ_1 near the mean-field value, $\gamma_{mf} = 1$ [35], for both ZFC and FC conditions (Table 1, lines s).
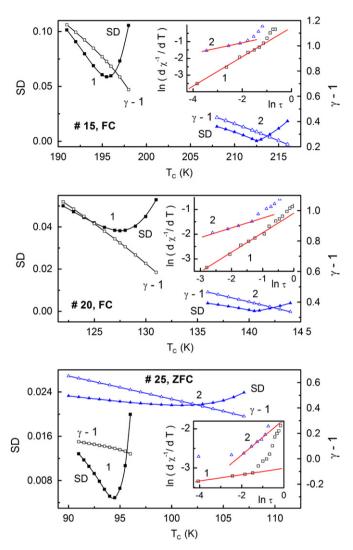

Fig. 5. The dependences of SD and $\gamma-1$ on T_C, obtained within the temperature intervals ΔT_1 (1) and ΔT_2 (2), with the second of Eq. (3). The lines are to guide the eye. Insets: the plots of $\ln(d\chi^{-1}/dT)$ (in arbitrary units) vs. $\ln \tau$ in the intervals ΔT_1 (1) and ΔT_2 (2) for the LSMFO samples at $B = 10$ G. The lines are linear fits.

Hence, the complex critical behavior of the susceptibility in #15 and #20 is consistent with coexistence of two different spin systems, namely the percolative system of large and strongly-correlated FM clusters and non-percolative (Heisenberg) system of small and weakly-correlated magnetic units. On the other hand, in #25 only the non-percolative processes influence the critical behavior of $\chi(T)$. This supports the preliminary conclusion, made in Section 2.3, about strong inhomogeneity of the magnetic state of LSMFO and the role of the spin systems above in formation of its FM and irreversible magnetic properties.

Similar coexistence of percolative and non-percolative (Heisenberg) processes influencing the critical behavior of $\chi(T)$, observed in thin films of $La_{1-x}Ca_xMnO_3$ [39] and bulk $La_{1-x}Ca_xMn_{1-y}Fe_yO_3$ [23] and $La_{1-x}Ba_xMnO_3$ [26], reflects the universality of the phase separation effect in manganite perovskites and related CMR compounds (Section 1). Following the same arguments as in [23,26,39], the volume fraction of the hole-rich FM phase, η, the mean magnetic moment of the FM particles, μ, and the concentration of the FM particles, n, can be estimated at the onset temperature of the critical percolation behavior, T_0, with the expressions $\ln(1-\eta) = [1+\tau(T_0)]^{-3} \ln(1-\eta_c)$, $\mu \approx 3\,kT_0\chi(T_0)/(M_s\eta)$ and $n \approx \eta M_s/\mu$, respectively, where $\eta_c \approx 0.29$ [40] and M_s is the saturation magnetization [23,26]. Then, typical values of the mean FM particle radius, r, and the correlation length, λ, of the critical percolation cluster at T_0 can be found with the equations $\eta = 1 - \exp(-4\pi n r^3/3)$ and $\lambda \approx R\tau(T_0)^{-\nu}$ [40], respectively, where $\nu \approx 1$ is the critical exponent of the correlation length and $R \approx 2\,(4\,\pi\,n/3)^{-1/3}$ [40]. Such estimations can be made only for #15 and #20, where the percolative critical behavior of $\chi(T)$ takes place (top and middle panels of Figs. 4 and 5), yielding the values of $\eta \approx 0.16$ and 0.11, $\mu \approx 0.9 \times 10^4\,\mu_B$ and $1.1 \times 10^4\,\mu_B$, $n \approx 1 \times 10^{18}\,cm^{-3}$ and $5 \times 10^{17}\,cm^{-3}$, $r \approx 3.4$ and 3.8 nm, and $\lambda/R_0 \approx 100$ and 70 for #15 and #20, respectively, where $R_0 = 2(4\pi N_0/3)^{-1/3}$ is the mean distance between the Mn sites. The large value of λ/R_0 agrees well with the onset of the percolative behavior, whereas also other parameters are reasonable and typical of the nanosize FM particles, found with macroscopic [23,26,39] and microscopic [12,41,42] methods in various CMR compounds.

3. Conclusions

The magnetic properties of ceramic LSMFO with $y = 0.15 - 0.25$ are investigated, paying special attention to the low-field ($B = 10$ G) behavior. The FM transition takes place at the Curie temperature, decreasing with y, which is connected to damping of the double-exchange FM interaction by doping with Fe. The magnetic irreversibility, observed along with the FM transition, reveals the frustrated ground state of LSMFO. Well above the FM transition the asymptotic

Table 1
Values of the critical temperatures $T_C^{(1)}$ and $T_C^{(2)}$ and the critical exponents γ_1 and γ_2, obtained within the optimum intervals ΔT_1 and ΔT_2, respectively, in the ZFC and FC cooling regimes with the first (f) and the second (s) of Eq. (3).

Sample	Case	$T_C^{(1)}$ (K)	γ_1	ΔT_1 (K)	$T_C^{(2)}$ (K)	γ_2	ΔT_2 (K)
#15	ZFC (f)	200.5 ± 1.5	1.81 ± 0.03	$210-230$	210 ± 2	1.31 ± 0.04	$230-249$
	ZFC (s)	197 ± 1	1.77 ± 0.07	$201-258$	210.5 ± 1.5	1.36 ± 0.02	$220-249$
	FC (f)	199 ± 1	1.86 ± 0.06	$208-268$	207 ± 1	1.42 ± 0.03	$230-259$
	FC (s)	195.5 ± 1.5	1.87 ± 0.04	$200-249$	212.5 ± 1.5	1.32 ± 0.03	$219-249$
#20	ZFC (f)	127 ± 1	1.80 ± 0.04	$140-191$	139 ± 1	1.39 ± 0.04	$147-161$
	ZFC (s)	129.5 ± 1.5	1.80 ± 0.04	$140-191$	141.5 ± 1.5	1.35 ± 0.04	$147-171$
	FC (f)	124.5 ± 1.0	1.81 ± 0.04	$135-185$	136 ± 2	1.45 ± 0.03	$151-185$
	FC (s)	127.5 ± 1.5	1.79 ± 0.06	$135-164$	140.5 ± 1.5	1.39 ± 0.02	$157-177$
#25	ZFC (f)	93 ± 2	1.01 ± 0.03	$103-118$	$-$	$-$	$-$
	ZFC (s)	94.5 ± 0.5	1.08 ± 0.03	$96-116$	101 ± 2	1.45 ± 0.03	$116-143$
	FC (f)	$-$	$-$	$-$	105 ± 2	1.22 ± 0.03	$113-144$
	FC (s)	92.5 ± 1.5	1.10 ± 0.02	$95-115$	102.5 ± 1.5	1.35 ± 0.02	$115-142$

Curie–Weiss dependence of $\chi(T)$ is observed with values of p_{eff} exceeding considerably those of single magnetic ions. The complex critical behavior of $\chi(T)$ near the FM transition reveals between $y = 0.15 - 0.20$ two different spin systems, the percolative and the non-percolative (Heisenberg). At $y = 0.25$ influence of the percolation process to the susceptibility is not observed, which is accompanied with increased magnetic irreversibility and suppression of the ferromagnetism. The dependence of $\chi(T)$ gives evidence for phase separation due to the generation of nanosize FM particles. The variation of the susceptibility with y suggests that the FM properties of LSMFO are governed mainly by the large and strongly-correlated percolative FM clusters, whereas the magnetic irreversibility and frustration in LSMFO can be explained by the system of weakly-correlated smaller magnetic units.

References

[1] R. von Helmolt, J. Wecker, B. Holzapfel, L. Schulz, K. Sammer, Phys. Rev. Lett. 71 (1993) 2331;
P. Schiffer, A.P. Ramirez, W. Bao, S.-W. Cheong, Phys. Rev. Lett. 75 (1995) 3336.
[2] Y. Moritomo, A. Asamitsu, Y. Tokura, Phys. Rev. B 56 (1997) 12190.
[3] J.M.D. Coey, M. Viret, S. von Molnar, Adv. Phys. 48 (1999) 167.
[4] P.-G. de Gennes, Phys. Rev. 118 (1960) 141;
K. Kubo, N. Ohata, J. Phys. Soc. Jpn. 33 (1972) 21.
[5] E. Dagotto, T. Hotta, A. Moreo, Phys. Rep. 344 (2001) 1.
[6] E. Dagotto, Nanoscale Phase Separation and Colossal Magnetoresistance, Springer-Verlag, Berlin, 2002.
[7] J. Blasco, J. Garcia, J.M. de Teresa, M.R. Ibarra, P.A. Algarabel, C. Marquina, J. Phys.: Condens. Matter 8 (1996) 7427.
[8] J.-S. Zhou, J.B. Goodenough, J.F. Mitchell, Phys. Rev. B 58 (1998) R 579.
[9] M.R. Ibarra, G.-M. Zhao, J.M. De Teresa, B. Garcia-Landa, Z. Arnold, C. Marquina, P.A. Algarabel, H. Keller, C. Ritter, Phys. Rev. B 57 (1998) 7446.
[10] M. Uehara, S. Mori, C.H. Chen, S.-W. Cheong, Nature 399 (1999) 560.
[11] M. Fäth, S. Freisem, A.A. Menovsky, Y. Tomioka, J. Aarts, J.A. Mydosh, Science 285 (1999) 1540.
[12] M. Hennion, F. Moussa, G. Biotteau, J. Rodriguez-Carvajal, L. Piusard, A. Revcolevschi, Phys. Rev. B 61 (2000) 9513.
[13] S.H. Chun, M.B. Salamon, Y. Tomioka, Y. Tokura, Phys. Rev. B 61 (2000) R9225.
[14] S.J.L. Billinge, R.G. Di Francesco, G.H. Kwei, J.J. Neumeier, J.D. Thompson, Phys. Rev. Lett. 77 (1996) 715.
[15] S.J.L. Billinge, Th. Proffen, V. Petkov, J.L. Sarrao, S. Kycia, Phys. Rev. B 62 (2000) 1203.
[16] A. Tiwari, K. Rajeev, J. Appl. Phys. 86 (1999) 5175.
[17] Q. Huang, Z.W. Li, J. Li, C.K. Ong, J. Appl. Phys. 89 (2001) 7410.
[18] K.B. Chashka, B. Fisher, J. Genossar, L. Patlagan, G.M. Reisner, Phys. Rev. B 63 (2001) 064403.
[19] O.Z. Yanchevskii, O.I. V'yunov, A.G. Belous, A.I. Tovstolytkin, Low Temp. Phys. 32 (2006) 134.
[20] V.P. Pashchenko, A.A. Shemyakov, A.V. Pashchenko, V.K. Prokopenko, Yu.F. Revenko, V.A. Turchenko, V.N. Varyukhin, V.P. D'yakonov, H. Szymczak, Low Temp. Phys. 33 (2007) 663.
[21] G.H. Jonker, Physica 20 (1954) 1118.
[22] K.H. Ahn, X.W. Wu, K. Liu, C.L. Chien, Phys. Rev. B 54 (1996) 15–299.
[23] R. Laiho, K.G. Lisunov, E. Lähderanta, J. Salminen, V.S. Zakhvalinskii, J. Magn. Magn. Mater. 250 (2002) 267.
[24] D. Chowdhury, Spin Glasses and Other Frustrated Systems, World Scientific, Singapore, 1986.
[25] R. Laiho, K.G. Lisunov, E. Lähderanta, P.A. Petrenko, J. Salminen, V.N. Stamov, V.S. Zakhvalinskii, J. Phys.: Condens. Matter 12 (2000) 5751;
R. Laiho, K.G. Lisunov, E. Lähderanta, P.A. Petrenko, V.N. Stamov, V.S. Zakhvalinskii, J. Magn. Magn. Mater. 213 (2000) 271;
R. Laiho, E. Lähderanta, J. Salminen, K.G. Lisunov, V.S. Zakhvalinskii, Phys. Rev. B 63 (2001) 094405.
[26] R. Laiho, K.G. Lisunov, E. Lähderanta, V.S. Zakhvalinskii, V.L. Kozhevnikov, I.A. Leonidov, E.B. Mitberg, M.V. Patrakeev, J. Magn. Magn. Mater. 293 (2005) 892.
[27] D.N.H. Nam, R. Mathieu, P. Nordblad, N.V. Khiem, N.X. Phuc, Phys. Rev. B 62 (2000) 1027.
[28] R. Mathieu, P. Nordblad, D.N.H. Nam, N.X. Phuc, N.V. Khiem, Phys. Rev. B 63 (2001) 174405.
[29] C.M. Varma, Phys. Rev. B 54 (1996) 7328.
[30] R. Laiho, K.G. Lisunov, E. Lähderanta, P.A. Petrenko, J. Salminen, V.N. Stamov, Yu.P. Stepanov, V.S. Zakhvalinskii, J. Phys. Chem. Solids 64 (2003) 2313.
[31] A. Yamamoto, K. Oda, J. Phys.: Condens. Matter 14 (2002) 1075.
[32] R. Laiho, K.G. Lisunov, E. Lähderanta, P.A. Petrenko, J. Salminen, M.A. Shakhov, M.O. Safontchik, V.S. Stamov, M.V. Shubnikov, V.S. Zakhvalinskii, J. Phys.: Condens. Matter 14 (2002) 8043.
[33] N. Belous, I. Zorin, N. Kulich, I. Lezhnenko, A. Tovstolytkin, Sov. Phys. Solid State 32 (1990) 887.
[34] E. Lähderanta, K. Eftimova, R. Laiho, H.Al. Kanani, J.C. Booth, J. Magn. Magn. Mater. 130 (1994) 23.
[35] H.E. Stanley, Introduction to Phase Transitions and Critical Phenomena, Clarendon, Oxford, 1971.
[36] A.G. Dunn, J.W. Essam, D.S. Ritchie, J. Phys. C 8 (1975) 4219.
[37] S. Kirkpatrick, Phys. Rev. Lett. 36 (1976) 69.
[38] J.C. Le Guillou, J. Zinn-Justin, Phys. Rev. Lett. 39 (1977) 95.
[39] H. Huhtinen, R. Laiho, E. Lähderanta, J. Salminen, K.G. Lisunov, V.S. Zakhvalinskii, J. Appl. Phys. 91 (2002) 7944.
[40] B.I. Shklovskii, A.L. Efros, Electronic Properties of Doped Semiconductors, Springer-Verlag, Berlin, 1984.
[41] M. Hennion, F. Moussa, G. Biotteau, J. Rodriguez-Carvajal, L. Piusard, A. Revcolevschi, Phys. Rev. Lett. 81 (1998) 1957.
[42] V. Chechersky, A. Nath, I. Isaac, J.P. Franck, K. Ghosh, H. Ju, R.L. Greene, Phys. Rev. B 59 (1999) 497.